

Internal Friction and Vulnerability of Mixed Alkali Glasses

Robby Peibst, Stephan Schott, and Philipp Maass

Institut für Physik, Technische Universität Ilmenau, 98684 Ilmenau, Germany

(Dated: February 24, 2005)

Based on a hopping model we show how the mixed alkali effect in glasses can be understood if only a small fraction α_V of the available sites for the mobile ions is vacant. In particular, we reproduce the peculiar behavior of the internal friction and the steep fall ("vulnerability") of the mobility of the majority ion upon small replacements by the minority ion. The single and mixed alkali internal friction peaks are caused by ion-vacancy and ion-ion exchange processes. If α_V is small, they can become comparable in height even at small mixing ratios. The large vulnerability is explained by a trapping of vacancies induced by the minority ions. Reasonable choices of model parameters yield typical behaviors found in experiments.

PACS numbers: 66.30.Dn, 66.30.Hs

The mixed alkali effect (MAE) is a key problem for understanding ion transport processes in glasses and refers to strong changes in transport properties upon mixing of two types of mobile ions (for reviews, see [1, 2]). Fundamental for the MAE is the behavior of the tracer diffusion coefficients D_A and D_B of two types of ions A and B. With increasing number fraction x of B ions, i.e. with successive replacement of A by B ions, D_A decreases while D_B increases. These changes are reflected in the activation energies $E_{A,B}(x) = k_B T \log D_{A,B}(x)$, so that at low temperatures $D_{A,B}(x)$ vary by many orders of magnitude. As a consequence, the ionic conductivity $\sigma(x) = (1-x)D_A(x) + xD_B(x)$ runs through a deep minimum close to the intersection point of D_A and D_B .

Much progress was made in the past to explain the MAE [3, 4, 5, 6, 7, 8, 9, 10, 11, 12]. EXAFS [13] and NMR measurements [14], and in particular recent analyses of neutron and x-ray scattering data with the reverse Monte Carlo technique [10] support the picture that a structural mismatch effect leads to distinct preferential diffusion pathways for each type of mobile ion. The connectivity and interference of these pathways determines the long-range ion mobilities. On this theoretical basis alone, however, main properties of the MAE are still not well understood.

One property is the large "vulnerability", that means the steep decrease of the diffusion coefficient of the majority ion, e.g. A, with beginning replacement by the minority ion B [15, 16]. In many mixed alkali glasses, $\ln D_A(x)$ is a convex function for small x , reflecting that $E_A(x)$ is a concave function in these systems [17, 18]. Why is the increase of E_A largest at beginning replacement, where the influence of the minority ion should be weak?

Another quantity poorly understood so far is the internal friction (for a review, see [19]). Measurements on mixed alkali glasses show that the ionic motion leads to two mechanical loss peaks, a single alkali peak (SP) and a mixed alkali peak (MP). The peak frequency ω_s^{-1} of the SP has (nearly) the same activation energy E_s as the diffusivity of the more mobile ion, while the lower peak

frequency ω_m^{-1} of the MP exhibits an activation energy E_m that is not simply related to that of the mobility of the less mobile ion. Particularly puzzling is that the height H_m of the MP can be comparable to the height H_s of the SP even at very small x , and that H_m becomes larger the more similar the two types of ions are [20].

In this Letter we show that these peculiar behaviors can be explained, if the fraction α_V of vacant sites for the mobile ions is small. Small values $\alpha_V = 5-10\%$ have been found recently in molecular dynamics simulations [21, 22], and should be expected also on general grounds, since empty sites correspond to local structural configuration of high energy [23]. Here we argue that the experimental results for the internal friction provide independent support for this feature.

To reason that conjecture, we note (see eq. (2) below) that the SP and MP can be attributed to processes, where the more mobile ions (e.g. A) exchange sites with vacancies (AV exchange), and where the A ions exchange sites with B ions (AB exchange). When denoting by $c_{A,B}$ the fractions of sites occupied by A, B ions, a mean-field argument then predicts that $H_s / c_A \alpha_V$ and $H_m / c_A c_B$ should become comparable if $\alpha_V \sim c_B$. Therefore, if it is possible to find $H_m \sim H_s$ at small x , where $c_B \sim x$ is small, α_V must be small also. Indeed, we will show in the following that this rough argument can be substantiated.

First we are confronted with the general problem whether the mismatch concept is sustainable as mechanism for the MAE if α_V is small. To this end we investigate a lattice model, where the rate w_{ij} for a jump of an ion ($= A, B$) from site i to a nearest neighbor site j is determined by the site and barrier energies

$$u_i = u_{mis,i}; \quad u_{ij} = u_0 + \frac{u_{mis}}{2} (u_i + u_j): \quad (1)$$

The mismatch effect is taken into account via the mismatch energies $u_i > 0$, $u_{mis} > 0$, and the structural variables $u_i, 0 \leq u_i \leq 1$ that specify the i -character of site i . A site i with large u_i has a local environment favorably accommodated to an A ion and hence a low

energy ϵ_i . Large values of A_i imply a small value of B_i and vice versa. This is accounted for by taking opposing mean values $A_i = 1$, B_i in the distributions of the i (see below). Below a threshold value ϵ_c , sites lose their identity and we require the energy to saturate ($\epsilon_i = \epsilon_{\text{mis}}^c$ for $i > \epsilon_c$).

The barriers u_{ij} in eq. (1) contain a bare structural barrier u_0 (characterizing the activation energy in the pure system s) and a mismatch barrier that becomes higher with increasing "foreign" (ϵ)-characters of the initial and target sites involved in a jump of an ion. This is necessary in order to obtain low mobilities for the minority ion in the dilute regime [24]. Within an Anderson-Stuart like picture [25] it can be physically understood by the fact that larger minority ions have to bring up an additional elastic strain energy when open up doorways, and that smaller minority ions have to surmount a higher saddle point energy associated with the Coulomb potential of the counter ions.

The disorder in the glass is reflected in the distributions of the ϵ_i . Due to the local accommodation of the network structure to the ions in course of the freezing process, the numbers of sites with large A_i and B_i scale with $(1-x)$ and x , respectively. In addition we take into account short-range correlation between the ϵ_i . A convenient (technical) way to generate corresponding distributions (the detailed form is not important here) is as follows: We draw ϵ_i from truncated Gaussians ($p(\epsilon_i)/\exp[-(\epsilon_i - \epsilon_i^0)^2/2\sigma^2]$ for $\epsilon_i \in [0;1]$ with $\epsilon_i^0 = \sum_j \epsilon_j/(z+1) = 1/2$, where the sum runs over site i and its nearest neighbors, and ϵ_j are random binary numbers equal to one with probability $(1-x)$.

Kinetic Monte Carlo simulations are performed in a simple cubic lattice with periodic boundary conditions, using Metropolis hopping rates $w_{ij} = \exp(-u_{ij}/k_B T) \min(1; \exp[-(\epsilon_j - \epsilon_i)/k_B T])$ (ϵ are attempt frequencies). We choose $\alpha_f = 0.05$ and consider, for computational convenience, a symmetric set of parameters $A_i = B_i$, $\epsilon_{\text{mis}} = \epsilon_{\text{mis}}^B = \epsilon_{\text{mis}}^A, \dots$ To determine the tracer diffusion coefficients and internal friction as functions of x and reduced temperature $k_B T = \epsilon_{\text{mis}}$, we fix the remaining parameters to $\epsilon_c = 2/7$, $\epsilon_{\text{mis}} = 1/14$, and $u_{\text{mis}} = 0.7 \epsilon_{\text{mis}}$. The parameter ϵ_{mis} characterizes the difference between the two types of mobile ions (e.g. with respect to size).

Figure 1a shows the normalized diffusion coefficient $D_A(x) = D_A(0)$ as a function of x for 5 different ϵ_{mis} (due to the symmetric parameters we do not plot $D_B(x) = D_A(1-x)$). The curves exhibit the typical behavior found in experiment: $D_A(x)$ decreases by many orders of magnitude when A ions are replaced by B ions. This effect becomes stronger with lower temperature or stronger difference ϵ_{mis} between the two types of mobile ions, i.e. with larger $k_B T = \epsilon_{\text{mis}}$. We thus conclude that the mismatch concept is sustainable for small α_f .

In particular, $\log[D_A(x)/D_A(0)] = -E_A(x)/k_B T$, ex-

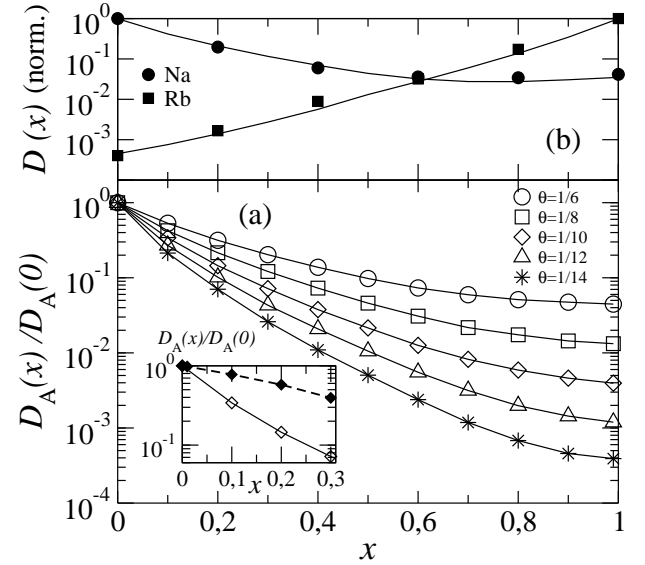


FIG. 1: (a) Normalized diffusion coefficient $D_A(x) = D_A(0)$ of A ions for 5 different reduced temperatures $\epsilon_{\text{mis}} = k_B T / \epsilon_{\text{mis}}$. The inset shows $D_A(x)$ for small x at $\epsilon_{\text{mis}} = 1/10$ (open symbols) in comparison with the results in the absence of a correlation induced trapping effect (full symbols). (b) Measured data (symbols) for $(1-x)\text{Na}_2\text{O}-x\text{Rb}_2\text{O}-4\text{B}_2\text{O}_3$ glasses at 652K (redrawn from [18]) and fit by the model (lines) with $\epsilon_{\text{mis}} = 1/9$ and asymmetric mismatch barriers $u_{\text{mis}}^B = 2u_{\text{mis}}^A = \epsilon_{\text{mis}}$.

hibits a convex curvature for small x , and $E_A(x)$ a concave curvature (see Fig. 4a; note that one must add u_0 to obtain the total activation energy $E_A^{\text{tot}}(x) = E_A(x) + u_0$). The large vulnerability is caused by a trapping effect: For small x , there exist regions in the glass where the network structure tended to accommodate to the "foreign" B ions. Because of the spatial correlations, the regions consist of several sites with smaller A_i character than on average. These sites are not only favorably occupied by B ions, but also favorably occupied by vacancies, because this allows more of the majority A ions to occupy well accommodated sites with large A_i close to one. Vacancies hence become trapped in regions more favourably accommodated to the foreign B ions and they have to bring up an additional activation energy to promote the diffusion of A ions. The corresponding reduction of $D_A(x)$ is strongest for $x \rightarrow 0$, since with increasing x the number of sites with values A_i close to one decreases. The importance of the trapping effect [26] is demonstrated in the inset of Fig. 1a, where $D_A(x)$ is shown in comparison with the curve obtained in the absence of spatial correlations ($A_i = A_i$ instead of $A_i = \sum_j \epsilon_j/(z+1)$) but otherwise the same parameters).

Fig. 1a resembles well the experimental behavior. By choosing asymmetric parameters one can reproduce measured curves as shown in Fig. 1b with reasonable parameter values (if we require $\epsilon_{\text{mis}} = 1/9$ in Fig. 1b to represent the experimental temperature 652K, we would obtain a mismatch energy $\epsilon_{\text{mis}} = 0.5\text{eV}$). A detailed fitting to ex-

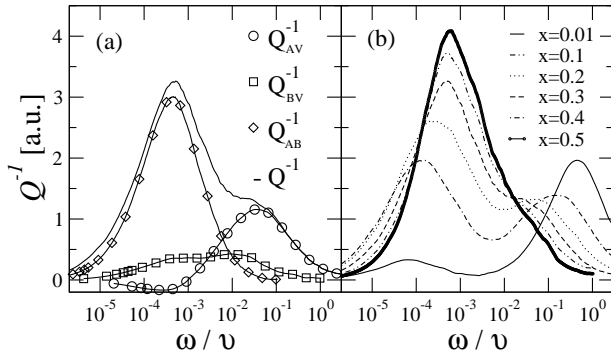


FIG. 2: (a) Internal friction Q^{-1} and spectral components (cf. eq. 2) as a function of ω for $x = 0.3$ and $T = 10$. (b) Change of the internal friction Q^{-1} with x for $T = 10$.

perimental results, however, is not our aim here (and has limitations due to the simplicity of the model).

Rather, we next explore how the behavior in the internal friction $Q^{-1}(\omega; T)$ can be understood. To this end, we consider a small modulation $\epsilon_i(t) = a_0 \exp[i\omega t]$ of the site energies in response to an oscillatory shear stress with amplitude a_0 and frequency ω [27]. The complex coupling constants ϵ_i fluctuate due to the disorder in the glass. Without making specific assumptions regarding their correlation properties, we employ a random phase ansatz and regard them to be uncorrelated for different sites i and different types α , $[\epsilon_i]_{av} = 0$ ($[\epsilon_i]_{av}$ denotes a disorder average). Introducing the occupation numbers $n_i(t)$, i.e. $n_i(t) = 1$ if site i is occupied by species α ($\alpha = A; B; V$ here) at time t and zero else, linear response theory then expresses the internal friction in terms of the Fourier cosine transforms of the exchange correlation functions $\langle n_i(t)n_j(0) \rangle$ ($\langle \cdot \rangle$ denotes a thermal average). The result is

$$Q^{-1}(\omega; T) = \frac{\omega}{k_B T} \sum_{i,j} \frac{c_{ij}}{Z} \frac{1}{\omega} \int_0^\infty dt C_{ij}(t) \cos(\omega t); \quad (2)$$

$$C_{ij}(t) = \langle n_i(t)n_j(0) \rangle / \langle n_i \rangle \langle n_j \rangle; \quad (3)$$

where c_{ij} is constant [28], $c_{ij} = \langle n_i n_j \rangle_{av}$, and $C_{ij}(t) = \langle n_i(t)n_j(0) \rangle / \langle n_i \rangle \langle n_j \rangle$ are the normalized exchange correlation functions [$C_{ij}(0) = 1$ and $C_{ij}(t \rightarrow \infty) = 0$].

Figure 2a shows Q^{-1} as a function of ω for $x = 0.3$ and $T = 10$, together with the spectral components Q_{AV}^{-1} , Q_{BV}^{-1} , Q_{AB}^{-1} in eq. (2). Two arise from exchange processes of the ions with the vacancies (AV and BV exchange) and one arises from exchange processes of the two types of ions (AB exchange). The exchange of vacancies with the majority ions (AV) leads to the SP and the AB exchange to the MP, while the BV exchange yields a broad spectral contribution that is masked by the SP and MP, and cannot be resolved in Q^{-1} . The overall behavior of Q^{-1} with varying x for $T = 10$ is shown in

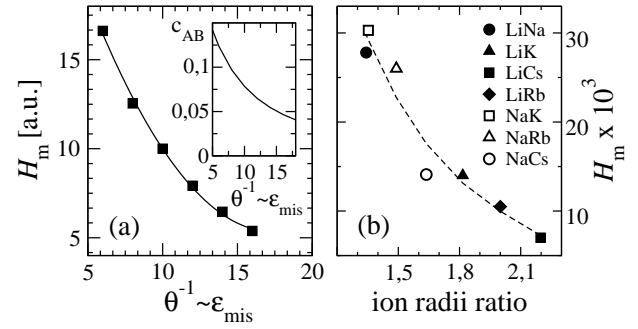


FIG. 3: (a) H_m in dependence of $\theta^{-1} = \omega_{mis}/k_B T$ at $x = 0.5$. The inset shows the decrease of c_{AB} with increasing $\theta^{-1} / \omega_{mis}$ (from analytical calculation). (b) H_m as a function of ion radii ratio of various mixed alkali pairs for $x = 0.5$ and $\omega = 0.4$ Hz fixed.

Fig. 2b. Due to the small c_{ij} , the MP can be well identified already for $x = 0.01$, in agreement with the argument given above. With increasing x the MP becomes higher and moves towards larger frequencies, while the SP becomes lower and moves towards smaller frequencies. At $x = 0.5$ the SP cannot be resolved any longer.

Remarkably, also the puzzling rise of the height H_m with increasing similarity of the two types of mobile ions (i.e. decreasing ω_{mis}) is reproduced, see Fig. 3a. H_m at $x = 0.5$ becomes higher with decreasing ω_{mis} (we regard T to be fixed here). The reason for this behavior lies in the weighting of the AB peak by the disorder averaged product $c_{AB} = \langle n_A^i n_B^i \rangle_{av}$ of the equilibrium occupations n_A^i , n_B^i in eq. (2). With increasing mismatch ω_{mis} , A and B ions share the same sites with lower probability (see inset of Fig. 3a) and accordingly H_m decreases. The behavior is reminiscent to the variation of H_m with the fraction of ion radii observed in experiments at $x = 0.5$ for a fixed frequency, see Fig. 3b [29].

When denoting by E_i the activation energies of the Q^{-1} peak frequencies ω_i , we can define by $E_s = \min(E_{AV}; E_{BV})$ and $E_m = E_{AB}$ the activation energies of the SP and MP. The activation energies E_i obtained from Arrhenius plots (for the same values as in Fig. 1) are shown in Fig. 4a together with the diffusion activation energies $E_{<} = \min(E_A; E_B)$ and $E_{>} = \max(E_A; E_B)$ of the more and less mobile ion. We find that $E_s (= \min(E_{AV}; E_{BV}))$ follows closely $E_{<}$, in agreement with measurements [19]. By contrast, $E_m (= E_{AB})$ differs from $E_{>}$. The deviations found in Fig. 4a are similar to those found in experiments, see Fig. 4b [30].

To show Q^{-1} as function of temperature for fixed frequency, as typically obtained in experiments, we use time-temperature scaling to transform Q^{-1} from frequency to temperature space. Taking the values from Fig. 1a, we first checked, that a scaling $\omega S(\omega; T) = F(\omega/T)$ is approximately valid. By applying this scaling we then replot Q^{-1} from Fig. 2b as function of T in Fig. 4c for small x and parameter values $\omega_{mis} = 1$ eV,

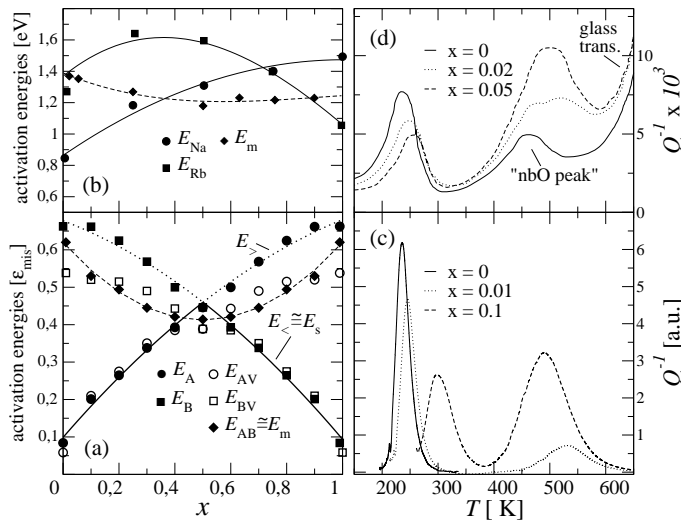


FIG. 4: (a) Activation energies of the tracer diffusion coefficients shown in Fig. 1, and of the spectral components of the internal friction. (b) E_{Na} , E_{Rb} , and E_m in $(1-x)Na_2O-xRb_2O-3SiO_2$ glasses (redrawn from [17]). (c) Q^{-1} calculated from Fig. 2 after applying time-temperature scaling for $m_{is} = 2u_0 = 1\text{eV}$ and $\omega = 10^{12}$ (see text). (d) Q^{-1} in $(1-x)Na_2O-xRb_2O-3SiO_2$ glasses for $\omega = 0.4\text{Hz}$ (redrawn from [17]).

$u_0 = 0.5\text{eV}$, and $\omega = 10^{12}$. These values yield activation energies $E_A^{\text{tot}}(x) = E_A + u_0$ of $0.6 \dots 1.2\text{eV}$ comparable to those found in experiments, cf. Fig. 4b. The choice $\omega = 10^{12}$ corresponds to $\omega' = 1\text{Hz}$, when $\omega' = 10^{12}\text{Hz}$ is a typical attempt frequency. Using this rough parameter estimate, peak temperatures in Fig. 4c are obtained that reflect the experimental scenario in Fig. 4d [note that the glass transition and the "non-bridging oxygen" (nbO) peak [19] are not taken into account in the present approach].

In summary, we have shown how the mixed alkali effect in glasses, including the vulnerability and the peculiar features of the internal friction, can be understood based on the mismatch effect in the presence of a small vacancy concentration. Due to the small α_i , H_m can become comparable to H_s even at small concentrations of the minority ion, and H_m increases, when it becomes easier for both types of ions to share the same sites. The large vulnerability can be connected to a trapping of vacancies induced by the minority ions. Reasonable choices of parameters allowed us to faithfully reproduce typical behaviors found in experiments.

We thank W. Dieterich, J. Habasaki, and M. D. Ingram for valuable discussions.

Electronic address: Philipp Maass@tu-ilmenau.de;

URL: <http://www.tu-ilmenau.de/theophys2>

[1] D. E. Day, J. Non-Cryst. Solids 21, 343 (1976).

- [2] M. D. Ingram, J. Non-Cryst. Solids 67, 151 (1994).
- [3] P. Maass, A. Bunde, and M. D. Ingram, Phys. Rev. Lett. 68, 3064 (1992); A. Bunde, M. D. Ingram, and P. Maass, J. Non-Cryst. Solids 172-174, 1222 (1994).
- [4] A. Hunt, J. Non-Cryst. Solids 175, 129 (1994).
- [5] G. N. Greaves and K. L. Ngai, Phys. Rev. B 52, 6358 (1995).
- [6] M. Tomozawa, Solid State Ionics 105, 249 (1998).
- [7] B. M. Schulz, M. Dubiel, and M. Schulz, J. Non-Cryst. Solids 241, 149 (1999).
- [8] P. Maass, J. Non-Cryst. Solids 255, 35 (1999).
- [9] R. Kirchheim, J. Non-Cryst. Solids 272, 85 (2000).
- [10] J. Swenson, A. Matic, C. Karlsson, L. Borjesson, C. Meneghini, and W. S. Howells, Phys. Rev. B 63, 132202 (2001).
- [11] J. Swenson and S. Adams, Phys. Rev. Lett. 90, 155507 (2003).
- [12] A. Bunde, M. D. Ingram, and S. Russ, Phys. Chem. Chem. Phys. 6, 3663 (2004).
- [13] G. N. Greaves et al., Phil. Mag. A 64, 1059 (1991).
- [14] B. Ge, M. Janssen, and H. Eckert, J. Non-Cryst. Solids 215, 41 (1997).
- [15] M. D. Ingram and B. Roling, J. Phys.: Condens. Matter 14, 1 (2002).
- [16] C. T. M. Oynihan and A. V. Lesikar, J. Am. Ceram. Soc. 63, 458 (1981).
- [17] G. L. McVay and D. E. Day, J. Am. Ceram. Soc. 53, 508 (1970).
- [18] S. Voss, A. W. Imre, and H. M. Ehrer, Phys. Chem. Chem. Phys. 6, 3669 (2004); S. Voss, F. Berkenzie, A. W. Imre, and H. M. Ehrer, Z. Phys. Chem. 218, 1353 (2004).
- [19] W. A. Zdzienicki, G. E. Rindone, and D. E. Day, J. Mater. Sci. 14, 763 (1979).
- [20] D. E. Day, in Amorphous Materials, eds. R. W. Douglas and B. Ellis (Wiley Interscience, New York, 1972), p. 39.
- [21] H. Lammer, M. Kunow, and A. Heuer, Phys. Rev. Lett. 90, 215901 (2003).
- [22] J. Habasaki and Y. Hiwatari, Phys. Rev. B 69, 144207 (2004).
- [23] J. C. Dyre, J. Non-Cryst. Solids 324, 192 (2003).
- [24] When a mismatch in the energy barriers is absent, the minority ions would, in the dilute limit, be driven away from their favorable low-energy sites by entropic forces and assume mobilities comparable to the majority ions.
- [25] O. L. Anderson and D. A. Stuart, J. Am. Ceram. Soc. 37, 573 (1954).
- [26] In the present model the trapping effect is caused by correlations in the structural properties. Alternatively, a trapping of vacancies can be caused by ion-ion interactions, as, for example, in the MAE seen in crystalline ionic conductors with ABO_3 structure [see M. Meyer et al., Phys. Rev. Lett. 76, 2338 (1996)].
- [27] D. K nodler, O. Stiller, and W. Dieterich, Phil. Mag. B 71, 661 (1995).
- [28] For the coefficient $\alpha = 2 \langle j_i j_j \rangle_{\text{av}} / M^0 a^3$, where M^0 is the real part of the shear modulus, which is governed by the (elastic) network response and thus very weakly dependent on frequency (α : mean jump distance).
- [29] When the ion ratio approaches one (as for the K/Rb pair), the correlation to m_{is} should become weaker and other properties (e.g. polarizabilities) will dominate m_{is} .
- [30] It is interesting to note that the activation energy corresponding to the exchange of vacancies with the less mo-

mobile ions does not follow the diffusion activation energy of the less mobile ion.